Comprehensive linear model for the n = m = 1 fishbone kinetic-MHD instability

G. Brochard, R. Dümont, X. Garbet, H. Lutjens, T. Nicolas, F. Orain

IOP Conf. Series: Journal of Physics: Conf. Series **1125** (2018) 012003 doi:10.1088/1742-6596/1125/1/012003

Comprehensive linear model for the $n = m = 1$ fishbone kinetic-MHD instability

G. Brochard[1], R. Dumont[1], X. Garbet[1], H. Lütjens[2], T. Nicolas[2], F. Orain[2]

[1] *CEA, IRFM, F-13108 Saint-Paul-lez-Durance, France*
[2] *CPhT, Ecole Polytechnique, F-91128 Palaiseau cedex, France*

E-mail: guillaume.brochard@cea.fr

Abstract. A comprehensive linear model for the interaction between the MHD $n = m = 1$ internal kink and fast particles, based on the Hamiltonian angle-action formalism, is derived. On the basis of this model, a linear code, MHD-K, that solves partially analytically and numerically the kinetic-MHD dispersion relation non-perturbatively is presented. The impact of passing fast particles on the fishbone is shown to be an essential drive of the instability, where previous models highlighted only trapped particles as the driver of the kinetic-MHD instability. Resonant planes in phase space are presented, showing multiple resonant branches for both trapped and passing particles.

1. Introduction

The kinetic-MHD fishbone instability has been studied extensively for the past three decades, from the experimental, theoretical and numerical points of views. First results of MHD bursts with the typical fishbone-like signature on magnetic oscillations were found at the PDX tokamak [1]. Since then, they have been observed in many other experiments [2][3] for different phase space distributionsof energetic particles. The relevance of studying this instability rests upon the fast particles transport, induced by the fishbone instability. The fast particles, such as the fusion born alpha particles, are transported out of the plasma core. This decreases the plasma performances due to a partial loss ofthe alphas heating, mandatory for steady-state plasma operations. Furthermore, such a transport can trigger disruptives MHD instabilities, such as NTMs (Neoclassical Tearing Modes). Due to the fact that future fusion devices such as ITER and DEMO are expected to produce a large quantity of alpha particles, understanding the interplay between kinetic suprathermic population and MHD both in itslinear and non-linear phase is crucial for conducting successful experiments. While the linear phase canbe investigated analytically for simple models, or with little numerical cost for more complete models,the study of the non-linear phase of the fishbone instability requires the use of complex numerical codes such as MEGA [4], M3D-K [5][6], XTOR-K[7][8]. However, for realistic non-linear predictions, such codes need to be firstly validated against complete linear model during their linear phase. The goal of this study is to provide analytical/numerical linear tools to perform such a validation, by derivinga complete linear model for the fishbone instability, and a linear code to solve the implicit dispersion relation. Using the formalism from [9], a more complete model is needed because, so far, theoreticallinear models [10],[11],[12],[13], primarily identified the precessionnal frequency of *trapped* energetic particles ω_d, as the drive of a resonant mechanism with the $n = m = 1$ internal kink mode, inducingthe fishbone instability. $\mathbf{v}_d$ is the magnetic drift velocity. It is argued in this paper that *passing* fast particles need to be considered as an equivalent drive to the fishbone instability. In later models [14]the contribution of passing particles has been taken into account, however the impact on the dynamicsof the fishbone has often been discarded, in some linear codes [5][15]. Moreover, some linear codes [16] compute perturbatively the fast particles contribution to the internal kink dispersion relation. Such an approximation holds for kinetic instabilities such as TAEs (Toroidal Alfven Eigenmodes). However, in the case of the fishbone, the growth rate of the instability can be up to one order of magnitudehigher for a given magnetic equilibrium on the fishbone branch than it is on the kink branch without

fast particles. That is why a non-perturbative treatment of the kinetic dispersion relation, implicit in complex frequency as it will be shown, is needed. This paper is organized as follows, in a first part, a comprehensive linear model for the fishbone instability is derived, through a Hamiltonian angle-action formalism that will be presented as well. In a second part, the linear code MHD-K that solves partly analytically and numerically the fishbone dispersion relation is presented, as well as linear results showing the relevance of passing particles on the instability due to multiple resonant planes in phase space associated with both passing and trapped particles.

2. Derivation of the linear model

2.1. Kinetic dispersion relation of the internal kink

Most linear models have used the energetic principle [17] to work out an expression for the fishbone dispersion relation with the additional functional introduced by kinetic populations : $\delta W_K = \int d^3\mathbf{x}d^3\mathbf{v}\, m_h\, \boldsymbol{\xi}\cdot\nabla\cdot(\mathbf{v}\otimes\mathbf{v})\tilde{f}_h$, $\tilde{f}_h$ the linear distribution response of energetic particles and $\boldsymbol{\xi}$ the MHD displacement. This kinetic term comes from the extra stress tensor Π_h due to fast particles in the momentum equation. Following what has been done in [18] and also in [19][20], the dispersion relation for the bi-fluid resistive internal kink mode $n = 1$, $m = 1$ is obtained by matching the expressions for ξ_r obtained from the linearized MHD equations, inside and outside of the inertial layer$q = 1$, yielding

$$D(n_{h0}, \omega) = \delta I(\omega) - i\omega_A[\lambda_H + \lambda_K(n_{h0}, \omega)] = 0 \tag{1}$$

$\omega \in \mathbb{C}$, with the inertial contribution δI given as

$$\delta I(\omega) = [3\omega(\omega-\omega_{*i})]^{1/2}\, I_R(\omega), \quad I_R(\omega) = \frac{8\Gamma\left(\frac{\Lambda^{3/2}+5}{4}\right)}{\Lambda_{9/4}\,\Gamma\left(\frac{\Lambda^{3/2}-1}{4}\right)}, \quad \Lambda = [\omega(\omega-\omega_{*i})(\omega-\omega_{*e})]^{1/3}\left(\frac{\tau_A}{S}\right)^{1/3}\frac{S}{s_0^2} \tag{2}$$

where ω_{*i}, ω_{*e} stands for the ion/electron-bulk diamagnetic frequency, ω the complex MHD mode frequency, S the Lundquist number, s_0 the magnetic shear at $q = 1$, ω_A the Alfvén pulsation, n_{h0} the density of fast particles on the magnetic axis, $\lambda_H = \gamma_{MHD}\tau_A$ the contribution of the bulk plasma, τ_A being the Alfvén time, and γ_{MHD} is the growth rate of the instability without fast particles, constant for a given MHD equilibrium. λ_K is a normalization of δW_K given by $\lambda_K = \mu_0\delta W_K/2\pi\xi_0^2 s_0 R_0 B_{\vartheta,0}^2$, with R_0 the major radius, $B_{\vartheta,0}$ the poloidal field at $q = 1$ and ξ_0 the constant radial MHD displacement. Here the eigenfunction $\boldsymbol{\xi}$ has been assumed to be a simple step function, null outside $q = 1$. The way (1) is solved will be discussed in the second part of the article. Firstly, the derivation of the kinetic term δW_K is presented. For this purpose, one needs to solve the Vlasov equation to work out an expression for the perturbed distribution of fast particles $\tilde{f}_h$.

2.2. Resolution of Vlasov equation

Let F_h be the distribution function of fast particles such as $F_h = F_{eq,h} + \tilde{f}_h$, with $F_{eq,h}$ being the equilibrium distribution function. Vlasov's equation can be written as, assuming no collisions

$$d_t F = \partial_t F - \{H, F\} = 0 \tag{3}$$

where $\{\cdot,\cdot\}$ are the the Poisson's brackets defined in an angle/action formalism [21] as

$$\{A, B\} = \frac{\partial A}{\partial\boldsymbol{\alpha}}\cdot\frac{\partial B}{\partial\mathbf{J}} - \frac{\partial B}{\partial\boldsymbol{\alpha}}\cdot\frac{\partial A}{\partial\mathbf{J}} \tag{4}$$

In a tokamak configuration, one can identify three invariants of motion J_i related to a set of conjugate fast varying angles $\boldsymbol{\alpha}_i$ [22],[23].The conjugate coordinates are given as follows

- (α_1, J_1) is related to the cyclotron motion, where α_1 stands for the gyroangle and J_1 is proportional to the magnetic moment μ
- (α_2, J_2) is related to the poloidal motion, where α_2 stands for the bounce angle and J_2 is a function of the two other invariants and the energy
- (α_3, J_3) is related to the toroidal motion, where $J_3 = P_\phi = mRv_\phi - e\psi(r)$ is the toroidal kinetic momentum, m and e the particle's mass and charge, v_ϕ its toroidal velocity and ψ the poloidal magnetic flux.

This set of coordinates has been built so that the equilibrium quantities are only functions of **J**, therefore the linearized equations of motion regarding the equilibrium Hamiltonian H_{eq}, where $H(\boldsymbol{\alpha}, \mathbf{J}) = H_{eq}(\mathbf{J}) + \tilde{h}(\boldsymbol{\alpha}, \mathbf{J})$, $\tilde{h}$ the perturbed hamiltonain, simply read

$$\frac{d\boldsymbol{\alpha}}{dt} = \frac{\partial H_{eq}}{\partial \mathbf{J}} = \boldsymbol{\Omega}, \qquad \frac{d\mathbf{J}}{dt} = -\frac{\partial H_{eq}}{\partial \boldsymbol{\alpha}} = 0 \tag{5}$$

Therefore, the unperturbed motion is characterized by three frequencies. $\Omega_1 = \omega_c$ is the gyrofrequency and Ω_2, Ω_3 are respectively the poloidal and toroidal transit frequency given by [21]

$$\Omega_2 = \omega_b = 2\pi \left(\int_{-\vartheta_0}^{\vartheta_0} \frac{d\vartheta}{I v_\parallel} \right)^{-1}, \qquad \Omega_3 = \delta_p q \omega_b + \omega_d \tag{6}$$

where ϑ_0 is the bounce angle, I the Jacobian for toroidal coordinates (ψ, ϑ, ϕ), ϑ the geometric poloidal angle, $v_\parallel$ the parallel velocity, δ_p is 1 for passing particles and 0 for trapped particles and ω_d the precessional frequency. Linearizing (3), one gets

$$\partial_t \tilde{f}_h - \{\tilde{h}, F_{eq,h}\} - \{H_{eq}, \tilde{f}_h\} = 0 \tag{7}$$

reducing, according to the definitions above, to

$$\partial_t \tilde{f}_h - \frac{\partial \tilde{h}}{\partial \boldsymbol{\alpha}} \cdot \frac{\partial F_{eq}}{\partial \mathbf{J}} + \frac{\partial \tilde{f}_h}{\partial \boldsymbol{\alpha}} \cdot \frac{\partial H_{eq}}{\partial \mathbf{J}} = 0 \tag{8}$$

since F_{eq} does not depend on angle variables, as it is an equilibrium quantity. Performing a Fourier expansion on the perturbed quantities, according to the defined angle/action variables, one has

$$\tilde{g} = \sum_{\mathbf{n}} g_{\mathbf{n}\omega} \, e^{i(\mathbf{n}\cdot\boldsymbol{\alpha} - \omega t)} \tag{9}$$

where $\mathbf{n} = (n_1, n_2, n_3)$ is linked to the angle/action formalism. Therefore, one readily obtains

$$\tilde{f}_{\mathbf{n}\omega} = -\frac{\mathbf{n} \cdot \partial F_{eq,h}/\partial \mathbf{J}}{\omega - \mathbf{n} \cdot \boldsymbol{\Omega}} \tilde{h}_{\mathbf{n}\omega} \tag{10}$$

Considering that $F_{eq,h}$ is solely a function of (H_{eq}, μ, P_ϕ), its derivative with respect to **J** expands as

$$\mathbf{n} \cdot \frac{\partial F_{eq,h}}{\partial \mathbf{J}} = \mathbf{n} \cdot \left(\frac{\partial H_{eq}}{\partial \mathbf{J}} \frac{\partial F_{eq}}{\partial H_{eq}} + \frac{\partial \mu}{\partial \mathbf{J}} \frac{\partial F_{eq}}{\partial \mu} + \frac{\partial P_\phi}{\partial \mathbf{J}} \frac{\partial F_{eq}}{\partial P_\phi} \right) = \frac{\partial F_{eq,h}}{\partial H_{eq}} \left[(\mathbf{n} \cdot \boldsymbol{\Omega} - \omega) + \omega_+ - \omega_* \right] \tag{11}$$

where ω is artificially introduced to later dissociate $\tilde{f}$ in resonant and fluid parts. ω_+ and ω_* are defined as

$$\omega_+ = n \frac{e_s}{m} \frac{\partial F_{eq,h}/\partial \mu}{\partial F_{eq,h}/\partial H_{eq}}, \qquad \omega_* = -n \frac{\partial F_{eq,h}/\partial P_\phi}{\partial F_{eq,h}/\partial H_{eq}} \tag{12}$$

with e_s the particle's charge and m the particle's mass. Considering the perturbed Hamiltonian, derived from the electromagnetic Lagrangian, assuming that the perpendicular potential vector $A_\perp$ can be discarded

$$\tilde{h} = e_s(\varphi - v_\parallel A_\parallel) \tag{13}$$

with φ the electric potential. Following the ideal MHD constraint on the system, $E_\parallel = 0$, and introducing the time integral of the electrical potential $\chi(\mathbf{x}, t) = \int_0^t \varphi(\mathbf{x}, t')dt'$, it leads to

$$E_\parallel = -\nabla_\parallel \varphi - \partial_t A_\parallel = 0 \Leftrightarrow A_\parallel = -\nabla_\parallel \chi \tag{14}$$

The perturbed Hamiltonian can then be expressed as

$$\tilde{h} = e_s[\partial_t \chi + v_\parallel \nabla_\parallel \chi] = e_s[d_t \chi - (\mathbf{v}_d \cdot \nabla)\chi] \tag{15}$$

where $d_t\chi = (\partial_t + \mathbf{v}\cdot\nabla)\chi$, $\mathbf{v} = v_\parallel\mathbf{b} + \mathbf{v}_d$, v_d being the drift velocity of fast particles. $d_t\chi$ can be expressed, using the angle-action Hamiltonian approach, as

$$d_t\chi = \partial_t\chi - \{H_{eq}, \chi\} = \partial_t\chi + \mathbf{\Omega}\cdot\frac{\partial\chi}{\partial\boldsymbol{\alpha}} \tag{16}$$

Therefore, plugging (16) into (15) and Fourier developping $\tilde{h}$, one gets

$$\tilde{h}_{\mathbf{n}\omega} = i(\mathbf{n}\cdot\mathbf{\Omega} - \omega)e_s\chi_{\mathbf{n}\omega} - [e_s(\mathbf{v}_d\cdot\nabla)\chi]_{\mathbf{n}\omega} \tag{17}$$

Then, inserting (17),(11) into (10), one obtains $\tilde{f}_{\mathbf{n}\omega} = \tilde{f}^{res}_{\mathbf{n}\omega} + \tilde{f}^{fl}_{\mathbf{n}\omega}$, with

$$\tilde{f}^{res}_{\mathbf{n}\omega} = \frac{\partial F_{eq}}{\partial H_{eq}}\frac{\omega - \omega_+ - \omega_*}{\omega - \mathbf{n}\cdot\mathbf{\Omega}}[e_s(\mathbf{v}_d\cdot\nabla)\chi]_{\mathbf{n}\omega}, \quad \tilde{f}^{fl}_{\mathbf{n}\omega} = \frac{\partial F_{eq}}{\partial H_{eq}}\left[i(\mathbf{n}\cdot\mathbf{\Omega} - \omega_+ - \omega_*)e_s\chi - [e_s(\mathbf{v}_d\cdot\nabla)\chi]\right]_{\mathbf{n}\omega} \tag{18}$$

Let us now introduce the ordering between the different resonant, diamagnetic and MHD frequencies for energetic particles. Ω_1 being generally several orders of magnitudes above Ω_2, Ω_3 and the pulsation of the internal kink ω, fast particles gyrofrequency cannot react resonantly with the MHD mode. It is then possible to reduce the number of resonances considering $n_1 = 0$. It implies also that $\omega_+ = 0$. Given that perturbed quantities such as the electrostatic potential are assumed to have, due to the internal kink, the following form $\varphi(r, \vartheta, \varphi) = \varphi(r)e^{-i(\vartheta-\phi)}$, their Fourier transform using angle-action formalism gives

$$\varphi_{\mathbf{n}} = \frac{1}{(2\pi)^2}\int d\alpha_2 d\alpha_3\, \varphi(r)e^{-i(\vartheta-\phi+n_3\alpha_3+n_2\alpha_2)} \tag{19}$$

Since $\alpha_3 = \phi - q\hat{\vartheta}$, with $\hat{\vartheta}$ a periodic function of α_2 defined in [21], and that $\vartheta = \hat{\vartheta} + \delta_p\alpha_2$, the only non vanishing component of $\varphi_{\mathbf{n}}$ following the integration over α_3 is $n_3 = n = 1$. Therefore, the general resonance condition reads

$$\omega - \sum_{n_2}\sigma_\parallel(n_2 + \delta_p q n)\omega_b - n\omega_d = 0 \tag{20}$$

$\sigma_\parallel = \pm 1$ for co/counter passing particles. Since the frequencies ω_b, ω_d depend on the three invariants of motion (E, P_ϕ, μ), the solutions of this resonance condition are surfaces in phase space. After numerical studies, which will be presented in part 3.3, for typical fast particles distribution and ITER-like MHD equilibrium, only three surfaces, one for trapped particles with $n_2 = 0$ and two for passing ones with $n_2 = -1$, mainly contribute to the resonant term, yielding for the $n = m = 1$ internal kink

$$\omega + \sigma_\parallel\delta_p(1 - q)\omega_b(E, P_\phi, \mu) - \omega_d(E, P_\phi, \mu) = 0 \tag{21}$$

Regarding the fluid term, it is not necessary to use the angle/action formalism, this formalism being better adapted to the study of resonant terms. It is therefore more convenient to express it in real space. Noticing that in Fourier space $\mathbf{v}\cdot\nabla = i\mathbf{n}\cdot\mathbf{\Omega}$ and that $\{\chi, P_\phi\} = in_3\chi_{\mathbf{n},\omega}$

$$\tilde{f}^{fl} = e_s\frac{\partial F_{eq}}{\partial H_{eq}}\left[v_\parallel\nabla_\parallel\chi - \omega_*\{\chi, P_\phi\}/n_3\right] \tag{22}$$

The first term of this expression is directly linked to the particle's tearing term in [9]. As a current term, it needs to be incorporated in δW_{MHD}, since it uses the total current, as shown is eq. (85-86) of [14].

In order to derive explicitly $\tilde{f}$, an expression of χ as a function of ξ_0, the order 0 MHD displacement, is needed. For $n = m = 1$, it reads $\boldsymbol{\xi} = \xi_0 H(r_{q=1} - \bar{r})e^{-i(\vartheta-\phi+\omega t)}\mathbf{e}_r$ at lowest order, where H is the Heaviside function and $\bar{r}$ a radial position linked to a specific choice of referent flux surface $\bar{\psi}$ [17][29]. Following reduced MHD assumption, at lowest order in $\epsilon = \bar{r}/R$ and assuming a toroidal equilibrium with concentric circular surfaces without Shafranov shift

$$\mathbf{v}_\perp = \mathbf{v}_{E\times B} \Leftrightarrow -i\omega\xi_0 B_0 e^{-i(\vartheta-\phi+\omega t)} = i\omega\partial_\vartheta\chi/\bar{r} \Leftrightarrow \chi = -i\xi_0 B_0\bar{r}e^{-i(\vartheta-\phi+\omega t)} \tag{23}$$

It is possible to obtain explicit expressions for both the resonant and fluid perturbed distribution using the definition of the drift velocity

$$\mathbf{v}_d = \frac{2E}{m\omega_c B}\mathbf{B}\times \quad 1-\frac{\lambda}{H}\ \boldsymbol{\kappa}+\frac{\lambda}{2H}\nabla \ln B \tag{24}$$

where $\lambda = \mu_0 B_0/H_{eq}$ stands for the generalized pitch angle, μ_0 being the order 0 magnetic moment and B_0 the magnetic field at $\bar{r}=0$, $H = R/R_0 = 1+\bar{r}/R_0\cos\vartheta$, ω_c the particle's gyrofrequency and $\boldsymbol{\kappa}$ the magnetic curvature. At low β, this expression reduces to

$$\mathbf{v}_d = \frac{E\sigma}{m\Omega BH}\mathbf{B}\times\nabla \ln B \tag{25}$$

with $B = B_0R_0/R$, $\sigma = 2-\lambda/H$ and $\mathbf{B} = (B_0/H)(\mathbf{e}_\varphi + (\bar{r}/Rq)\mathbf{e}_\vartheta)$. Therefore

$$\nabla \ln B = \left[\frac{\sin\vartheta}{R_0}\mathbf{e}_{\vartheta} - \frac{\cos\vartheta}{R_0}\mathbf{e}_{r}\right] \tag{26}$$

Then

$$\mathbf{v}_d\cdot\nabla = -\frac{\sigma E}{e_s B_0 R_0}\left[\sin\vartheta\partial_r + \frac{\cos\vartheta}{\bar{r}}\partial_\vartheta\right] \tag{27}$$

For the resonant term, one has

$$(\mathbf{v}_d\cdot\nabla)\chi = \frac{\sigma E\xi_0}{e_s R_0}e^{i(\alpha_3+q\hat{\vartheta}-\omega t)} \tag{28}$$

The Fourier coefficient being given by the inverse Fourier transformation

$$g_{\mathbf{n}\omega} = \int \frac{d\alpha_1}{2\pi}\frac{d\alpha_2}{2\pi}\frac{d\alpha_3}{2\pi}e^{-i\mathbf{n}\cdot\boldsymbol{\alpha}}g \tag{29}$$

two cases need to be considered in computing the resonant term. Firstly, for trapped particles, as will be shown numerically in part 3.3 for the n=m=1 internal kink, only the triplet $\mathbf{n}_t = (0, 0, 1)$ contributes, therefore

$$[e_s(\mathbf{v}_d\cdot\nabla)\chi]_{\mathbf{n}_t\omega} = \frac{E\xi_0}{R}\int\frac{d\alpha_2}{2\pi}\sigma e^{iq\vartheta} = \frac{E\xi_0}{R}\sigma I^q \tag{30}$$

where $I_q = <\cos\vartheta>_{\alpha_2} + (1-q)<\vartheta\sin\vartheta>_{\alpha_2}$, whose derivation is given in annex. For passing particles, only the triplet $\mathbf{n}_p = (0, -1, 1)$ is contributes, therefore

$$[e_s(\mathbf{v}_d\cdot\nabla)\chi]_{\mathbf{n}_p\omega} = \frac{E\xi_0}{R}\int\frac{d\alpha_2}{2\pi}\sigma e^{iq\vartheta+(1-q)\alpha_2} = \frac{E\xi_0}{R}\sigma I_{q,p} \tag{31}$$

Given the α_2 dependency in $I_{q,p}$, the obtention of an analytical expression for it is quite intricated. However, performing a serie expansion of $\exp[(1-q)\alpha_2]$, where $1-q$ is considered as a small parameter given that the studied MHD instability is the internal kink, trapped and passing contributions are identical at lowest order. Therefore the analytical expression for I_q is used for both trapped and passing particles. The resonant perturbed distribution function then reads

$$\tilde{f}^{res}_{\mathbf{n}\omega} = E\frac{\partial F_{eq}}{\partial H_{eq}}\frac{\omega-\omega^*}{\omega+\delta_p\sigma_\parallel(1-q)\omega_b-\omega_d}\frac{\xi_0}{R_0}I^q(r,\lambda) \tag{32}$$

Regarding the fluid term, using the expression of Poisson's brackets in regular toroidal coordinates [24], one finds

$$\{\chi, P_\phi\} = -\frac{\mathbf{b}}{eB_0}\cdot\nabla\chi\times\nabla P_\phi = \frac{\bar{r}}{q}\hat{r}\cdot(\mathbf{b}\times\nabla\chi) \tag{33}$$

where $P_\phi = cst = -e\bar{\psi} = -e\bar{r}^2B_0/2q$, assuming thin orbits around the magnetic surfaces and $q(\bar{r})$ almost constant inside $q=1$. The choice $\bar{\psi} = \psi + mRv_\phi/Ze$ is explained in the next section. The fluid contribution, or interchange contribution by comparison with [9], yields

$$\tilde{f}^{int} = -\xi_0 \frac{\partial F_{eq}}{\partial \bar{r}} e^{i(\phi-\vartheta)} \tag{34}$$

where one can see that the adiabatic contribution from [12] is retrieved, as well as the more general expression in eq. (71) of [14] in the limit of thin particles orbits.

2.3. Derivation of the toroidal drift frequency ω_d

To retrieve an expression for ω_d, one needs to express the toroidal angle as $\phi = \omega_3 t + F(\alpha_2)$, where ω_3 is the pulsation associated with the third angle of the angle-action formalism, and F is a periodic function of α_2. Given the angle α from the Clebsch magnetic field expression, $\alpha = \phi - q(\psi)\vartheta$; and that any angle ξ respects $\xi = \mathbf{v} \cdot \nabla = (v_\parallel \nabla_\parallel + \mathbf{v}_d \cdot \nabla)\xi$

$$\dot{\alpha} = \mathbf{v}_d \cdot \nabla \phi - q(\bar{\psi})\vartheta - \frac{dq}{d\psi}(\bar{\psi})\hat{\psi}\vartheta \tag{35}$$

where $\bar{\psi}$ stands for the referent flux surface for a given particle orbit, an invariant as a function of invariants. $\hat{\psi}$ stands for the excursion from $\bar{\psi}$ along the orbit, such as $\psi = \bar{\psi} + \hat{\psi}$. Given that $\bar{\psi}$ is an unperturbed quantity, and that $\hat{\psi}$ is a first order quantity, as well as $\mathbf{v}_d \cdot \nabla\vartheta$, at leading order

$$\dot{\alpha} = \mathbf{v}_d \cdot \nabla\phi - q(\bar{\psi})\mathbf{v}_d \cdot \nabla\vartheta - \frac{dq}{d\psi}(\bar{\psi})\vartheta\mathbf{v}_d \cdot \nabla\hat{\psi} \tag{36}$$

Noticing that $\vartheta\mathbf{v}_d \cdot \nabla\hat{\psi} = \vartheta(d\hat{\psi}/dt) = d(\vartheta\hat{\psi})/dt - (d\vartheta/dt)\hat{\psi}$

$$\dot{\alpha} = \mathbf{v}_d \cdot \nabla\phi - q(\bar{\psi})\mathbf{v}_d \cdot \nabla\vartheta + \frac{dq}{d\psi}(\bar{\psi})\hat{\psi}\frac{d\vartheta}{dt} - \frac{dq}{d\psi}(\bar{\psi})\overline{\frac{d(\hat{\psi}\vartheta)}{dt}} \tag{37}$$

Then, performing an averaging over α_2, and a series expansion in $q(\psi)$ regarding the toroidal angle, ϕ can be written as

$$\phi = (\omega_d + \delta_p q(\bar{\psi})\omega_b)t + \delta_p q(\bar{\psi})\hat{\vartheta}(\alpha_2) + \chi(\alpha_2) \tag{38}$$

where the toroidal drift frequency is given by

$$\omega_d = \mathbf{v}_d \cdot \nabla\phi - \bar{q}(\bar{\psi})\mathbf{v}_d \cdot \nabla\vartheta + \frac{dq}{d\psi}(\bar{\psi})\hat{\psi}\frac{d\vartheta}{dt}_{\alpha_2}, \qquad \chi(\alpha_2) = \int_0^t dt'[\dot{\alpha} - <\dot{\alpha}>_{\alpha_2}] \tag{39}$$

Since $\delta_p\hat{\vartheta}(\alpha_2) + \chi(\alpha_2)$ is a periodic function of α_2, $\omega_3 = \omega_d + \delta_p q(\bar{\psi})\omega_b$ and ω_d is well defined. This expression for ω_d is identical to the one used in [25], eq. 10. However, it has been chosen here to work with $\bar{\psi}$ rather than ψ, since the resonance is solely a function of the invariants, which simplify the analytical/numerical computation of δW_K.

Though, it should be noted that such a choice for $\bar{\psi}$ does not allow all the physics related the inertial layer to be retained, since the MHD displacement $\boldsymbol{\xi}$ is naturally a function of ψ, not $\bar{\psi}$. Therefore, using a step function for $\boldsymbol{\xi}$, inertial enhancement and global stability effects recovered in [25], where ψ was chosen as radial variable, are not included in our model. However, for fast particles at low energies ($\sim 100keV$), orbit width are relatively small, which means that considering $\boldsymbol{\xi}(r) = \boldsymbol{\xi}(\bar{r})$ should not impact significantly the solution of the kinetic eigenvalue problem.

The change of variable has been chosen as $P_\phi \rightarrow \bar{\psi} = -P_\phi/Ze$, $\hat{\psi} = mRv_\parallel/Ze$, such as $\bar{\psi}$ stands for the flux surface at the tips of the banana orbits for trapped particles. One should note that such a change of variable is arbitrary, allowable for all classes of particles and simplify expressions. The toroidal drift frequency therefore yields, at leading order in ϵ

$$\omega_d = \frac{q(\bar{r})E\lambda}{Ze\bar{r}R_0B_0}I_d, \quad I_d = <\cos\vartheta>_{\alpha_2} + s(\bar{r})\frac{m}{\epsilon\lambda E} <v_\parallel^2>_{\alpha_2} \tag{40}$$

where I_d is given in annex.

2.4. Derivation of δW_K

Using the energy principle, the kinetic contribution to (1) is given by

$$\delta W_K = \frac{1}{2}\int_V d^3\mathbf{x}\, \boldsymbol{\xi}^* \cdot \nabla \cdot \boldsymbol{\Pi}_h \tag{41}$$

where $\mathbf{\Pi}$ stands for the stress tensor. Considering the equation of motion for fast particles, discarding their inertia on the basis of their dilution in the whole plasma, $\mathbf{J}_h \times \mathbf{B} = \nabla \cdot \mathbf{\Pi}_h$. Since $\boldsymbol{\xi} = (\mathbf{b}/B) \times \nabla \boldsymbol{\chi}$, δW_K can be rewritten as, using vectorial identities

$$\delta W_K = -\frac{1}{2} \int d^3\mathbf{x}\, \mathbf{J}_{\perp h} \cdot \nabla \boldsymbol{\chi}^*, \qquad \mathbf{J}_{\perp h} \equiv \int d^3\mathbf{v} F_h e_s \mathbf{v}_d \tag{42}$$

$\mathbf{J}_{\perp h}$ being the perpendicular hot current. It should be noted here that the parallel component of the hot particles current has also to be taken into account, this term being incorporated into the functionnal δW_{MHD} so that the current considered in Maxwell equations stands for the total current, as it should. Using the same normalization as in the previous part

$$\lambda_K = \frac{1}{\xi_0^2 s_0 R_0 B_p} \int d^3\mathbf{x} d^3\mathbf{v} F_h [e(\mathbf{v}_d \cdot \nabla)\boldsymbol{\chi}^*] \tag{43}$$

Therefore, using this expression, the resonant perturbation in Fourier space and applying Parseval's theorem

$$\lambda_K = \frac{1}{s_0 R_0 B_p^2} \int d^3\mathbf{x} d^3\mathbf{v} \frac{\partial F_{eq}}{\partial E} \frac{\omega - \omega_*}{\omega + \delta_b \sigma_\parallel (1-q)\omega_d - \omega} \frac{\sigma^2 E^2}{R^2 I_q^2} \tag{44}$$

The strategy that has been adopted to obtain precise numerical results for λ_K is to solve analytically the energy/velocity integral and numerically the others. This is due to the fact that the resonances depend on all integration variables. Therefore, computing the resonant integral analytically enhances the overall precision of λ_K. This strategy here differs from others linear codes such as [16] that use a grid adapted to the resonance patterns expected in the plane (ψ, E). Therefore, in order to carry outsuch an analytical integration, one needs to express the resonant term as an unitary polynomial of Eor v. Then, expliciting ω_*^{res}

$$\lambda_K = \frac{1}{s_0 R_0 B_p^2} \int d^3\mathbf{x} d^3\mathbf{v} \frac{\sigma E^2 I^2}{R^2 I_d^q} \frac{\partial F_{eq}}{\partial \bar{r}} \frac{R}{E_\alpha} - \frac{\partial F_{eq}}{\partial \hat{E}} \frac{x\hat{\omega}}{q} \frac{1}{\hat{E} + \delta_b^p \sigma_\parallel (1-q) E_0^0 \hat{\omega}_b \hat{E}^{1/2} - E_0^0 \hat{\omega}} \tag{45}$$

where $\hat{E} = E/E_\alpha$, $\hat{v} = v/v_\alpha$, $\hat{\omega} = \omega/\bar{\omega}_d$, $\bar{\omega}_d = \omega_d[\bar{r} = r_0, \lambda = (1-\epsilon_0)^{-1}, E = E_\alpha] = E_\alpha/e_s B_0 r_0 R_0$, $r_0 = r_{q=1}$,$x = \bar{r}/r_0$ $E_0 = x/q\sigma I_d$, $\hat{\omega}_b = 2e_s B_0 r_0/q m_\alpha v_\alpha I_{b,p}$, and where $\sigma_\parallel = \pm 1$ regarding co-passing/counter-passing particles. The interchange term reads

$$\lambda_K^{int} = -\frac{1}{s_0 R_0 B_p} \int d^3\mathbf{x} d^3\mathbf{v} \frac{\partial F_{eq}}{\partial \bar{r}} \frac{\sigma E}{R} e^{-i\vartheta} \tag{46}$$

One now needs an expression for the volume element in phase space using the coordinates$(\bar{r}, \vartheta, \varphi, E, \lambda, \Phi)$, Φ being the gyro-angle. In toroidal geometry, assuming large aspect ratio and using $(v_\parallel, v_\perp, \Phi)$ coordinates

$$\int d^3\mathbf{x} = 2\pi R_0 \int_0^a \bar{r} d\bar{r} \int_0^{2\pi} d\vartheta, \qquad \int d^3v = \int 2\pi v_\perp dv_\parallel dv_\perp = 2\pi \int \sum_\sigma E^{1/2} \left(\frac{2}{m}\right)^{1/2} \left(\frac{\lambda}{H}\right)^{1/2} \mathbf{J}\, dE d\lambda \tag{47}$$

where $\sigma_\parallel = sgn(v_\parallel)$, $\mathbf{J}$ is the Jacobian of the change of variable $(v_\parallel, v_\perp) \rightarrow (E, \lambda)$. Since $v_\parallel = \sigma_\parallel (2E/m)^{1/2}(1 - \lambda/H)^{1/2}$, $v_\perp = (2\lambda E/mH)^{1/2}$, one has the following derivatives

$$\frac{\partial v_\parallel}{\partial E} = \sigma_\parallel (2Em)^{-1/2}(1-\lambda/H)^{1/2}, \qquad \frac{\partial v_\parallel}{\partial \lambda} = -\sigma_\parallel (2Em)^{1/2} (2H)^{-1}(1-\lambda/H)^{-1/2} \tag{48}$$

$$\frac{\partial v_\perp}{\partial E} = (\lambda/2mEH)^{1/2}, \qquad \frac{\partial v_\perp}{\partial \lambda} = (E/2m\lambda H)^{1/2} \tag{49}$$

yielding

$$\frac{\partial E}{\partial \lambda} = J = \frac{1}{2m\,(\lambda H)^{1/2}(1-\lambda/H)^{1/2}} \tag{50}$$

Therefore, using the following identity, phase space in our set of variables is expressed as

$$\int_{-\pi}^{\pi} d\vartheta \int_{0}^{H} d\lambda = \int_{0}^{(1-\epsilon)^{-1}} d\lambda \int_{-\vartheta_0}^{\vartheta_0} d\vartheta \tag{51}$$

$$\int d^3\mathbf{x}d^3\mathbf{v} = \sum_{\sigma_\parallel=\pm 1} \pi^2 R_0 \left(\frac{2}{m}\right)^{3/2} \int_0^{r_0} \bar{r}d\bar{r} \int_0^{(1-\epsilon)^{-1}} d\lambda \int_{-\vartheta_0}^{\vartheta_0} \left|1-\frac{\lambda}{H}\right|^{-1/2} d\vartheta \int_0^{\infty} E^{1/2} dE \tag{52}$$

where the sum over the parallel velocity is two for trapped particles. Regarding the different terms of λ_K, considering only even terms in ϑ and the bounce-averaging formalism developed, one gets

$$\lambda_K^{res} = \frac{2\pi^3\epsilon}{s_0 r_0 B_{0,p}} \left(\frac{2}{m}\right)^{3/2} \sum_{\sigma_\parallel=\pm 1} \int_0^{r_0} \bar{r}d\bar{r} \int_0^{(1-\epsilon)^{-1}} d\lambda \sigma I_b \frac{I_q^2}{I_0^{2,p}} \int_0^{\infty} E^{5/2} \frac{\partial_{\bar{r}} F_{eq}/E\alpha - \bar{r}\hat{\omega}\partial_{E} F_{eq}/qr_0 R_{0,p\parallel}}{\hat{E}+\delta\,\sigma\,(1-q)E\,|\hat{\Omega}\quad|\hat{E}^{1/2}-E\,\hat{\omega}} dE \tag{53}$$

$$\lambda_K^{int} = -\frac{4\pi^3\epsilon_0}{s_0 r_0 B_{p,0}} \left(\frac{2}{m}\right)^{3/2} \int_0^{r_0} \bar{r}d\bar{r} \int_0^{(1-\epsilon)^{-1}} d\lambda \sigma I_b I \int_0^{\infty} E^{3/2} \frac{\partial F_{eq}}{\partial \bar{r}} dE \tag{54}$$

where $I_c = <\cos\vartheta>_{\alpha_2}$, $I_b = <1>_{\alpha_2}$. After little algebra, one can show that these two expressions are identical to δW_1 and δW_2 [14]. This re-derivation has been done to obtain expressions suited for analytical/numerical computation. Since an analytical treatment is preferred for the energy integral, calculations have to be specific to a given equilibrium particles distribution function, which is done for an isotropic slowing-down distribution function in Appendix B. Now that the kinetic term has been derived, let us discuss the resolution of the dispersion relation

3. Resolution of the dispersion relation with MHD-K and linear results

3.1. MHD-K

The linear code MHD-K solves equation (1) using a partial analytical approach. λ_K is integrated over all phase space, however, as it was shown, its integrand only depends on the triplet $(\bar{r}, E, \lambda)$. As shown in Appendix B, given an equilibrium function for fast particles, one can solve analyticallythe energy integral. Such an analytical treatment of the resonance brings a great deal of precision in the computation of λ_K. This is due to the fact that a 3D grid would have been inaccurate, the polesof the integrand being multiple and dependent on the triplet $(\bar{r}, E, \lambda)$. The other integrals over the pitch-angle and radial position are solved numerically using elliptic integrals of the first and second kind, as presented in Appendix A.

The fluid term $\lambda_H = \gamma_{MHD}\tau_A$ of the dispersion relation is calculated using the coupled codes CHEASE [26], that computes the 3D toroidal MHD equilibrium and XTOR-2F [27], that time iterates the equilibrium through the bi-fluid resistive extended MHD equations. All equilibrium quantities and profiles used in MHD-K are directly taken from CHEASE. It is important to note that γ_{MHD} is the linear growth rate computed by XTOR-2F for a given equilibrium in absence of fast particles. Therefore, it is assumed that the fast particle current is negligible regarding the total current. Fluid contributions are therefore not counted twice, since the total current response is present in δW_{MHD}, and the fast particles' pressure response in δW_K [14].

MHD-K assumes, as does the linear model, that the equilibrium has concentric circular magnetic flux surfaces without Shafranov shift. Therefore, CHEASE is used with circular plasma cross section. However with circular flux surfaces, a Shafranov shift is always present when solving Grad-Shafranov equation. This is handled in MHD-K by shifting its geometric axis to the magnetic axis of CHEASE, assuming a larger major radius than expected.

Then, (1) is solved through a method somewhat simpler than in [28]. Since the goal of the linear code is to verify non-linear hybrid kinetic-MHD codes, it is not necessary to use a complex algorithm locating the zeros of an analytic function. Instead, the value of the kinetic term λ_K is computed ona 2D grid

in the complex plane (ω, γ), then $1/|D(n_{h,0}, \omega + i\gamma)|^2$ is computed all over the grid, its maximum being considered as the solution of (1) for a given kinetic density on the magnetic axis $n_{h,0}$.

By taking the maximum of $1/|D(n_{h,0}, \omega + i\gamma)|^2$ as the solution of (1), it is assumed that the solutions are unique, which is not necessarily the case. In fact, it has been observed that for the internal kink in presence of fast particles, two branches co-exist. The kink branch at low fast particles density, and the fishbone branch at high density. But since the kink and fishbone branches are stabilized respectively at high and low density, only one branch exists in the unstable region $\gamma > 0$. Only the unstable solutions are of interest, since the goal of MHD-K is to be used as a tool to verify hybrid codes, where only unstable modes can exist.

3.2. Effects of passing particles on the fishbone mode

In the following, linear results obtained from MHD-K are presented. These results have been obtained from an ITER-like equilibrium with $R_0 = 6.2m, B_0 = 5.3T, a = 1.86m, S = 1.10^7, \omega_{*i} = 0$, parabolic-like q profile with $q_0 = 0.8$ on the magnetic axis. Bulk and fast particles profiles have the form $P = P_0(1 - r^{\alpha})^{\beta}$, where for the bulk density n_i, $n_{i,0} = 2.10^{19}m^{-3}$, $\alpha = \beta = 2$, for the bulk temperature T_i, $T_{i,0} = 30keV, \alpha = \beta = 2$ and for the fast particles density n_h, $n_{h,0}$ is a parameter and $\alpha = 2, \beta = 6$.

The fast particles are distributed along an isotropic slowing-down equilibrium distribution function, as presented in Appendix B. The peak energy of the particle is set to $E_{\alpha} = 3.5MeV$, which is the energy of fusion-born alphas. In later comparison with hybrid codes, this peak energy might be decreased for precise comparisons between the linear model and numerical results. At high energy, $1MeV$, particles follow non-standard orbits known as potato orbits [29], as the particle's orbit width increases with its energy. However, it has been assumed in the linear model that particles follows thin banana orbits, therefore lower energies $\sim 100keV$ would be preferred.

By varying $n_{h,0}$ from 0 to $12.10^{17}m^{-3}$, results shown in Figure 1 have been obtained Considering

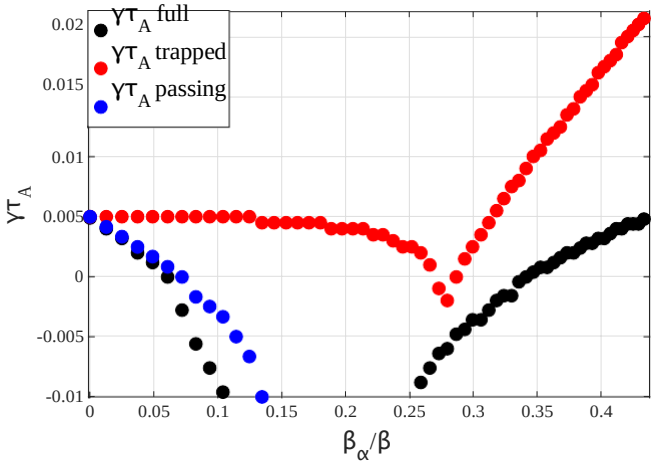

Figure 1: *Linear growth rate of the kinetic kink instability, β_{α} the fast particles beta on the magnetic axis, considering respectively all particles, only passing particles and only trapped particles*

the full model curve in Figure 1, one can see that the typical behavior for the kinetic kink instability is retrieved. At low fast particles density, the internal kink is stabilized and then, past a threshold in β_{α}, $\beta_{\alpha}/\beta \sim 0.35$ here, the fishbone mode is dominant and the kink instability is destabilized.

The variation of γ regarding n_{h0} needs to be explained here. This variation is due to two competing physical effects. By looking closely at (1), assuming $\omega_{*i} = 0$, $\gamma\tau_A = \gamma_{MHD}\tau_A + n_{h0}Re[\tilde{\lambda}_K(\omega + i\gamma)]$, $\tilde{\lambda}_K = \lambda_K/n_{h0}$. Only a variation of the real part of λ_K can explain the variation of γ. As it can be seen on Figure 2, the overall (trapped and passing particles) fluid term inside $Re[\lambda_K]$ is due to the negative density gradient and the mostly positive sign of I_c in the (ψ, λ) plane. Therefore it is not the one producing the stabilization. The real resonant term $Re[\lambda_K^{res}]$ is mostly negative in phase space

according to the sign of I_d. Then, the stabilization is produced by the non-reactive part, a fluid-like effect of $Re[\lambda^{res}_K]$, since at low frequency it can be shown that in most of the phase space $Re(\omega) = \mathbf{n}\,\mathbf{\Omega}_i$. When the fast particles density is increased, this fluid-like effect competes with the resonant effect, because there are now significant zones of the phase space where $Re(\omega) = \mathbf{n}\,\mathbf{\Omega}$, leading to the desta- bilization. This variation of $Re[\lambda^{res}_K]$ is illustrated in Figure 2. Physically, it can be explained by the fact that at low density, the fast particles behave mostly as a fluid since few particles occupy the small regions in which they interact resonantly with the MHD mode. As the density is increased, more particles occupy the resonant zones, leading to a prevalence of the resonant effect on to the fluid effect.

It can also be seen on Figure 1 that passing particles have a significant effect on the fishbone mode, since the results of the full model are not retrieved when only considering trapped particles. This can firstly be explained by the fact that fluid terms from passing particles are of the same order of magnitude as for the trapped particles, as shown in Figure 2. Secondly, as it will be shown in the following part, the MHD mode also reacts resonantly with passing particles. This is also illustrated

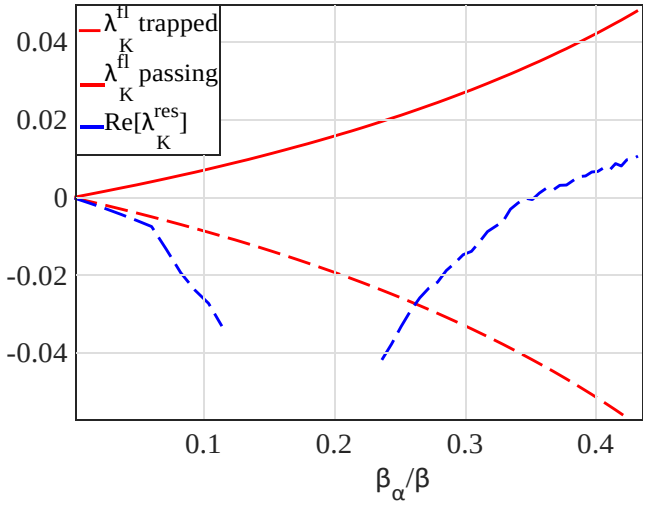

Figure 2: *Comparison of fluid and real resonant part of the kinetic term, underlying the competitive physical effects*

by Figure 3, where the pulsation of the MHD mode is presented for the three models. When solely considering passing or trapped particles, the MHD mode frequency is not as high as it is when all classes of particles are considered. This due to the fact that the kink instability has less resonant interactions with the energetic particles, which implies that resonant surfaces also exist inside the passing part of phase space.

3.3. Resonances plane in phase space

In Figure 4, the resonance curves at a fixed radial position $\bar{r} = 0.8\, r_{q=1}$ are displayed. They are obtained by plotting the integrand of δW_K in the 3D space $(\bar{r}, E, \lambda)$. Regarding (20), only two particle modes contribute here, $\mathbf{n} = (0, 1, 1)$ for passing particles and $\mathbf{n} = (0, 0, 1)$ for trapped particles. Inthe phase space zone concerned by passing particles, two different resonant curves, associated with the same particle mode, can be seen. They correspond to the co-passing and counter passing contributionsto the mode. Regarding the amplitude of the curves, in most cases, the trapped curve has an amplitudeup to five times higher that passing curves. However, passing curves usually cover a broader area in phase space. Therefore, this result underlines the necessity to consider passing particles in the linear model to properly describe the kinetic internal kink mode, since depending on the imposed equilibrium function in phase space, the resonant effects could be due entirely to passing particles.

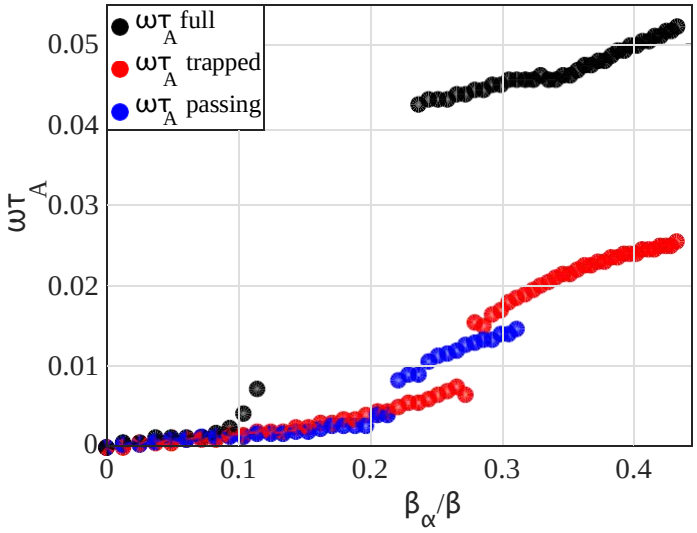

Figure 3: *Linear pulsation of the kinetic kink instability, β_α the fast particles beta on the magnetix axis , considering respectively all particles, only passing particles and only trapped particles*

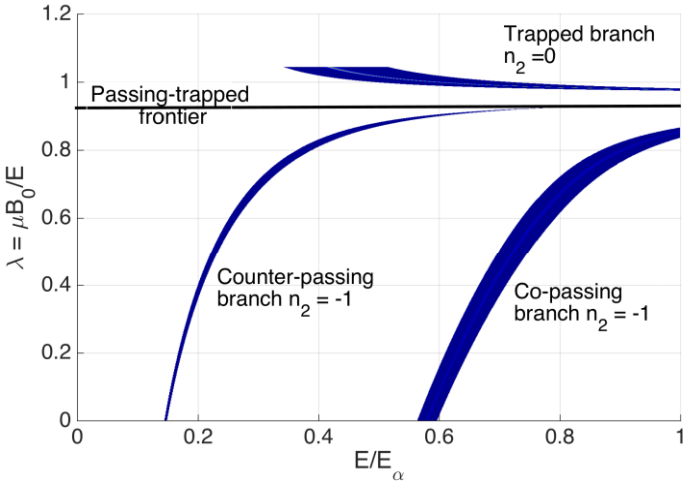

Figure 4: *Resonant curves in the (E, λ) plane, for a fixed radial position $\bar{r} = 0.8 r_0$, r_0 being the $q = 1$ radius*

4. Conclusion

A new linear model, including more physical effects than some previous ones, has been derived here using a Hamiltonian angle-action formalism. On its basis, the linear code MHD-K has been developed, solving non-pertubatively the kinetic internal kink dispersion relation. The linear results obtained from MHD-K have shown the relevance of considering passing particles in linear models, since they are also a resonant drive to the emergence of the fishbone mode. This new linear tool aims at testing non-linear hybrid kinetic codes during their linear phase, in order to verify their correct implementation. Such a verification is currently underway with the code XTOR-K [7][8], a hybrid kinetic-MHD using for the MHD part the solver from [27], and for the kinetic part a 6D PIC module.

This work has been carried out within the framework of the French Research Federation for Fusion Studies, and of the EUROfusion Consortium. It has received funding from the Euratom research

and training programme 2014-2018 under grant agreement No 633053 for the project WP17-ENR- CEA-06. This work is part of the project AMICI funded by the Agence Nationale pour la Recherche (ANR-14-CE32-0004-01). The views and opinions expressed herein do not necessarily reflect those of the European Commission.

Appendix A. Bounce-averaging formalism

In this section, bounce-averaging calculations are detailed for both passing and trapped particles. Any bounce-averaged quantity $< F >$ is calculated through

$$< F >= \int_C \frac{F}{v_\parallel} dl \Big/ \int_C \frac{dl}{v_\parallel} \tag{A.1}$$

where C is the path followed by the particle. The parallel velocity can be expressed as follows, considering $E = 1/2mv^2$, $\mu = mv_\perp^2/2B$, $\lambda = \mu B_0/E$, $H = R/R_0$

$$v_\parallel = \left(\frac{2E}{m}\right)^{1/2} \left(1 - \frac{\lambda}{H}\right)^{1/2} \tag{A.2}$$

Assuming circular flux surfaces, it yields, for ϑ_0 the bounce angle for trapped particles and $\vartheta_0 = \pi$ for passing ones

$$< F >= \int_{-\vartheta_0}^{\vartheta_0} F \left(1 - \frac{\lambda}{H}\right)^{-1/2} \frac{d\vartheta}{2\pi} \Big/ \int_{-\vartheta_0}^{\vartheta_0} \left(1 - \frac{\lambda}{H}\right)^{-1/2} \frac{d\vartheta}{2\pi} \tag{A.3}$$

using $\epsilon = r/R_0$, one has

$$\left(1 - \frac{\lambda}{H}\right)^{-1/2} = (1 - \lambda + \epsilon\lambda)^{-1/2} \left(1 - \frac{\sin^2(\vartheta/2)}{y^2}\right)^{-1/2} \tag{A.4}$$

with y^2 being expressed as

$$y^2(x, \lambda) = \frac{1 - \lambda + \epsilon\lambda}{2\epsilon\lambda} \tag{A.5}$$

It can be noted that [12] uses a different definition for y^2. One can distinguish passing from trapped particles by a simple condition on y^2. Trapped particles are characterized by the existence of two turning points in the poloidal plane where their parallel velocity is null. Therefore, the condition on having trapped particles translates itself, according to (A.2), as $(1 - \lambda/H)^{1/2} = 0$, which implies, assuming $\lambda < 1/1 - \epsilon$, that $0 < y^2 < 1$. Passing particles are therefore characterized by $1 < y^2 < +\infty$.

From these conditions on y^2, one can deduce the corresponding conditions on the pitch angle λ. Respectively, for $y^2 = 0, 1, +\infty$, the corresponding λ are $\lambda = 1/1 - \epsilon$, $\lambda = 1/1 + \epsilon$, $\lambda = 0$. Therefore, for trapped particles, $1/1 + \epsilon < \lambda < 1/1 - \epsilon$, and for passing particles, $0 < \lambda < 1/1 + \epsilon$.

These expressions enable to write $< F >$ as

$$< F >= \int_{-\vartheta_0}^{\vartheta_0} F \left(1 - y^{-2} \sin^2(\vartheta/2)\right)^{-1/2} \frac{d\vartheta}{2\pi} \Big/ \int_{-\vartheta_0}^{\vartheta_0} \left(1 - y^{-2} \sin^2(\vartheta/2)\right)^{-1/2} \frac{d\vartheta}{2\pi} \tag{A.6}$$

Let us now derive expressions for $< \cos\vartheta >$, $< \vartheta \sin\vartheta >$, $< v_\parallel^2 >$ and $< \cos(q\vartheta) >$ for both passing and trapped particles, which are appearing in the derivation of λ_K.

Appendix A.1. Passing particles

For passing particles, $\vartheta_0 = \pi$, the frequency to perform a poloidal revolution is defined as

$$\frac{\omega_b}{2\pi} = \frac{(2E/m)^{1/2}}{qR_0 I_{b,p}} \tag{A.7}$$

where

$$I_{b,p} = \int_{-\pi}^{\pi} \left(1 - \frac{\lambda}{H}\right)^{-1/2} \frac{d\vartheta}{2\pi} = 4(1-\lambda+\epsilon\lambda)^{-1/2} \int_0^{\pi/2} (1 - y^{-2}\sin^2\vartheta)^{-1/2} \frac{d\vartheta}{2\pi} = (1-\lambda+\epsilon\lambda)^{-1/2} \frac{2\mathrm{K}(1/y^2)}{\pi} \tag{A.8}$$

K being the elliptic integral of first kind. The definition of a bounce-averaged quantity is then straightforward

$$< F(\vartheta) >_P = \int_0^{\pi/2} \frac{F(2\vartheta)(1 - y^{-2}\sin^2\vartheta)^{-1/2}}{\mathrm{K}(1/y^2)} d\vartheta \tag{A.9}$$

Therefore, knowing that

$$\cos 2\vartheta = 1 - 2\sin^2\vartheta = 2y^2\left(1 - \frac{1}{y^2}\sin^2\vartheta\right) + 1 - 2y^2 \tag{A.10}$$

one has

$$< \cos\vartheta >_P = I_{c,p} = 2y^2 \frac{\mathrm{E}(1/y^2)}{\mathrm{K}(1/y^2)} + 1 - 2y^2 \tag{A.11}$$

where E is the elliptic integral of the second kind. Moreover, noticing that

$$\partial_\vartheta \left[- 4y^2(1 - y^{-2}\sin^2\vartheta)^{1/2} \right] = 2\sin 2\vartheta(1 - y^{-2}\sin^2\vartheta)^{-1/2} \tag{A.12}$$

it implies, using an integration by parts

$$\int_0^{\pi/2} 2\vartheta \sin 2\vartheta(1 - y^{-2}\sin^2\vartheta)^{-1/2} d\vartheta = \left[- 4y^2\vartheta(1 - y^{-2}\sin^2\vartheta)^{1/2} \right]_0^{\pi/2} + 4y^2 \int_0^{\pi/2} (1 - y^{-2}\sin^2\vartheta)^{1/2} d\vartheta \tag{A.13}$$

Therefore, it yields

$$< \vartheta\sin\vartheta >_P = I_{s,p} = 4y^2 \frac{\mathrm{E}(1/y^2)}{\mathrm{K}(1/y^2)} - \frac{\pi}{2\mathrm{K}(1/y^2)}(1 - y^{-2}) \tag{A.14}$$

For $< v_\parallel^2 >$, the derivation is straightforward

$$< v_\parallel^2 > = \frac{4E\lambda\epsilon y^2}{m} \frac{\mathrm{E}(1/y^2)}{\mathrm{K}(1/y^2)} \tag{A.15}$$

Finally, in order to obtain $< \cos(q\vartheta) >_P$, one simply performs an expansion according to the small paramater $(1 - q)$, reading

$$< \cos(q\vartheta) >_P = I_{q,p} = < \cos\vartheta >_P + (1 - q) < \vartheta\sin\vartheta >_P = I_{c,p} + (1 - q) I_{s,p} \tag{A.16}$$

Appendix A.2. Trapped particles

For trapped particles, ϑ_0 can have any value in the interval $[0, \pi]$. In order to have explicit expressions for bounce-averaged terms, one needs to perform a change of variable. Considering the following one, $(1/y)\sin(\vartheta/2) = \sin u$, $d\vartheta = 2y/\cos(\vartheta/2)\ \cos u\ du$ and knowing that $\cos(\vartheta/2) = (1 - y^2\sin^2 u)^{1/2}$, and also noticing that $\vartheta \in [-\vartheta_0, \vartheta_0] \to u \in [-\pi/2, \pi/2]$ since the existence of a bounce angle implies that $y^2 = \sin^2\vartheta_0/2$, one has

$$I_{b,t} = \int_{-\vartheta_0}^{\vartheta_0} \left(1 - \frac{\lambda}{H}\right)^{-1/2} \frac{d\vartheta}{2\pi} = \int_{-\pi/2}^{\pi/2} \frac{4y\ du}{\cos(\vartheta/2)\, 2\pi} = \frac{r}{R_0}\lambda^{-1/2} \frac{2\mathrm{K}(y^2)}{\pi} \tag{A.17}$$

where the bounce frequency is given in this case by

$$\omega_b = (2E/m)^{1/2}$$

$$\pi \qquad 2qR_0 I_{b,t} \tag{A.18}$$

Moreover, knowing that $\cos\vartheta = 2(1 - y^2\sin^2 u) - 1$

$$\int_{-\vartheta_0}^{\vartheta_0} \cos\vartheta \left(1 - \frac{\lambda}{H}\right)^{-1/2} d\vartheta = 4\left(2\lambda\frac{r}{R_0}\right)^{-1/2} \int_0^{\pi/2} \frac{\cos\vartheta}{\cos(\vartheta/2)} du = 4\left(2\lambda\frac{r}{R_0}\right)^{-1/2} [2\mathrm{E}(y^2) - \mathrm{K}(y^2)] \quad \text{(A.19)}$$

which gives

$$< \cos\vartheta >_T = I_{c,t} = 2\frac{\mathrm{E}(y^2)}{\mathrm{K}(y^2)} - 1 \quad \text{(A.20)}$$

Performing the same integration by parts as before for $< \vartheta\sin\vartheta >_T$, where this time the first term is dropped since $1 - y^{-2}\sin^2\vartheta_0/2 = 0$

$$\int_{-\vartheta_0}^{\vartheta_0} \vartheta\sin\vartheta \left(1 - \frac{\lambda}{H}\right)^{-1/2} d\vartheta = 4\left(2\lambda\frac{r}{R_0}\right)^{-1/2} 4y^2 \int_{-\vartheta_0}^{\vartheta_0} 1 - y^{-2}\sin^2(\vartheta/2)^{1/2} d\vartheta \quad \text{(A.21)}$$

Therefore, noticing that $\cos^2 u = y^{-2}(1 - y^2\sin^2 u) + 1 - y^{-2}$

$$< \vartheta\sin\vartheta >_T = I_{s,t} = \frac{4y^2}{\mathrm{K}(y^2)} \int_0^{\pi/2} \frac{\cos^2 u}{(1 - y^2\sin^2 u)^{1/2}} du = 4\frac{\mathrm{E}(y^2)}{\mathrm{K}(y^2)} + 4(y^2 - 1) \quad \text{(A.22)}$$

For $< v_\parallel^2 >$, it can be shown easily, using the same expression for $\cos^2 u$, that

$$< v_\parallel^2 >= \frac{E\lambda\epsilon}{m} < \vartheta\sin\vartheta > \quad \text{(A.23)}$$

The expression of $< \cos q\vartheta >$ is defined identically for both passing and trapped particles.

Appendix B. Kinetic contribution using a slowing down distribution

Using a normalized slowing-down distribution function, different from [12]

$$F_{eq}(\bar{r}, v) = \frac{3}{4\pi \ln[1 + (v_\alpha/v_c)^3]} \left(\frac{m}{2}\right)^{3/2} n(r) \frac{\vartheta(v_\alpha - v)}{v^3 + v_c^3} \quad \text{(B.1)}$$

with v_c the critical speed at which fast particles give out as much energy to bulk ions and electrons, expressed as, with m_h the mass of hot particles

$$v_c^3(\bar{r}) = \frac{3\sqrt{\pi}}{4}\frac{m_e}{m_h}\left(\frac{2T_e(\bar{r})}{m}\right)^{3/2} \quad \text{(B.2)}$$

Considering the following change of variable $\hat{E} = \hat{v}^2$ in order to express the resonance as a second order polynom, it yields, for the main contribution to λ'^{res}_K proportional to ω_*, using $v_1 = (1 - q)|\hat{\Omega}_2|$

$$\lambda^{res,\omega_*} = \frac{3\pi^2\epsilon_0 E_\alpha}{\kappa\, 2s_0 r_0 B^2 \ln[1 + (v_\alpha/v_c)^3]} \sum_{p,0} \int_{\sigma_\parallel=\pm 1} dn_\alpha \bar{r} d\bar{r} \int_0^{r_0} d\bar{r} \int_{(1-\epsilon)^{-1}} d\lambda \sigma I_b \frac{I_q^2}{I_d} \int_0^1 \frac{2\hat{v}^3}{\hat{v}^2 + \delta_p\sigma_\parallel E_0 v_1 \hat{v} - E_0\hat{\omega}} d\hat{v} \quad \text{(B.3)}$$

It should be noted that from the term $1/(v^3 + v_c^3)$, only the contribution $1/v^3$ has been kept. This is a reasonable approximation for highly energetic particles, such as fusion born alphas, since in this case $(v_c/v_\alpha)^3 \sim 10^{-1}$. For fast particles with lower energies ($\sim 100keV$), the reverse needs to be done.

One now needs to identify the resonant roots, that are functions of the considered $(\bar{r}, \lambda)$ couple. Given the usual determinant $\Delta = E_0[\delta_p E_0 v_1^2 + 4\hat{\omega}]$, the roots yields

$$\hat{v}_\pm(r, \lambda) = \frac{-\delta_p\sigma_\parallel v_1(\bar{r}, \lambda)E_0(\bar{r}, \lambda) \pm \sqrt{\Delta(\bar{r}, \lambda)}}{2}$$

(B.4)

In the general case, the roots are complex, since $|\nu_1 E_0| \sim 1$ for $1 - q \sim 10^{-1}$, with opposed imaginary parts. It should be noted that for ITER like equilibrium and $1 - q \sim 10^{-1}$, $(1 - q)\omega_{*e} \sim \omega_{*i}$ in the

particular case of trapped particles, the roots are simply given by $\pm\sqrt{E_0\hat{\omega}}$. Then, using these roots, one can perform a decomposition in simple elements, which yields, after straightforward algebra

$$\int_0^1 \frac{2\hat{v}^3}{\hat{v}^2+\delta\sigma_{p\parallel 0}E_0\hat{v}-E_0\hat{\omega}}d\hat{v} = \frac{2}{\hat{v}_+-\hat{v}_-}\left[\hat{v}_-\int_0^1\frac{\hat{v}^2}{\hat{v}-\hat{v}_-}d\hat{v}-\hat{v}_+\int_0^1\frac{\hat{v}^2}{\hat{v}-\hat{v}_+}d\hat{v}\right] \quad (B.5)$$

which expands to

$$\int_0^1 \frac{2\hat{v}^3}{\hat{v}^2+\delta\sigma_{p\parallel 0}E_0\hat{v}-E_0\hat{\omega}}d\hat{v} = \frac{2}{\hat{v}_+-\hat{v}_-}\times \left[\hat{v}_-\left(\frac{1}{2}+\hat{v}_-\right)\left(1+\hat{v}_-\ln\left(1-\frac{1}{\hat{v}}\right)\right)-\hat{v}_+\left(\frac{1}{2}+\hat{v}_+\right)+\hat{v}_+\ln\left(1-\frac{1}{\hat{v}}\right)\right] \quad (B.6)$$

When computing this integral, one needs to handle carefully the complex logarithm cut-off. When varying $(\bar{r},\lambda)$ to solve the remaining integrals, the resonant roots need to vary continuously. For a cut-off located on the negative part of the real axis in the complex plane, it can be shown that the cut off happens when $Im(v_\pm)$ switches sign while $Re(1-1/v_\pm)<0$. Since the complex logarithm is given by $\ln_C z = \ln|z| + 2i\arctan(Im(z)/[Re(z)+\frac{1}{2}])$, a factor $\pm 2i\pi$ is added to the complex logarithm when the poles are crossing the cut off half axis, the sign depending on the crossing direction.

The resonant term has been divided in two parts regarding the diamagnetic frequency and the mode frequency. The contribution proportional to the mode frequency is supposed to be lower than the other, but it is derived here anyway

$$\lambda_K^{res,\hat{\omega}} = \frac{3\pi^2\epsilon_0^2\hat{\omega}E_\alpha}{2s_0B_{p,0}\ln[1+(v_\alpha/v_c)^3]}\sum_{\sigma_\parallel=\pm 1}\int_0^{r_0}\frac{x^2n_\alpha}{q}d\bar{r}\int_0^{(1-\epsilon)^{-1}}\frac{I^2}{I^q}d\lambda\sigma I_b \times\left[\frac{1}{1+\delta\sigma_{p\parallel 0}E_0\hat{v}-E_0\bar{\omega}}+\frac{3}{2}\int_0^1\frac{\hat{v}}{\hat{v}^2+\delta\sigma_{p\parallel 0}E_0\hat{v}-E_0\bar{\omega}}d\hat{v}\right] \quad (B.7)$$

with

$$\int_0^1\frac{\hat{v}d\hat{v}}{\hat{v}^2+\delta\sigma_{p\parallel 0}E_0\hat{v}-E_0\hat{\omega}} = \frac{1}{\hat{v}_+-\hat{v}_-}\times\left[\hat{v}_-\ln(1-1/\hat{v}_-)-\hat{v}_+\ln(1-1/\hat{v}_+)\right] \quad (B.8)$$

The interchange term simply reads

$$\lambda_K^{int} = -\frac{3\pi^2\epsilon_0E_\alpha}{s_0r_0B_{p0}\ln[1+(v_\alpha/v_c)^3]}\int_0^{r_0}\frac{dn_\alpha}{d\bar{r}}\bar{r}d\bar{r}\int_0^{(1-\epsilon)^{-1}}\frac{I^2}{I^q}\sigma I_b d\lambda \quad (B.9)$$

[1] K. McGuire and al, PRL, 50, 12 (1983)
[2] M. Nave and al, Nuclear Fusion, Vol.31, No.4 (1991)
[3] M. J. Mantsinen and al, Plasma Phys. Control. Fusion 42 (2000) 1291-1308
[4] Y. Pei, N. Xiang, Y. Hu, Y. Todo, G. Li, W. Shen, L. Xu, Physics of Plasmas 24, 032507 (2017)
[5] G. Y. Fu and al, Physics of Plasmas 13, 052517 (2006)
[6] F. Wang, G. Y. Fu, J. A. Breslau, J. Y. Liu, Physics of Plasmas 20, 102506 (2013)
[7] D. Leblond, PhD thesis, (2011)
[8] H. Lutjens and al, Description of the hybrid code XTOR-K, to be submitted (2018)
[9] D.Edery, X.Garbet, J-P.Roubin, A.Samain (1992), PPCF, 34, 6, 1089-1112
[10] L. Chen, R. B. White, M. N. Rosenbluth, PRL, 52, 13, (1984)
[11] R. B. White, F. Romanelli and M. N. Bussac, Phys. Fluids B 2, 745 (1990); doi: 10.1063/1.859312
[12] Coppi, B., S. Migliuolo, F. Pegoraro and F. Porcelli (1990). *Phys. Fluids* B2, 927
[13] F. Porcelli, PPCF, 33, 13 1601-1620, (1991)
[14] F. Porcelli, R. Stankiewicz, W. Kerner, H.L. Berk (1994) *Physics of Plasmas*, 1,470
[15] C. Z. Cheng Physics Reports 211, No. 1 (1992) 1-51. North-Holland

[16] F. Nabais and al. Plasma Science and Technology, Vol.17, No.2, Feb. 2015
[17] Freidberg, J. (2014). Ideal MHD. Cambridge: Cambridge University Press. doi:10.1017/CBO9780511795046
[18] B. Coppi, R. J. Hastie, S. Migliuolo, F. Pegoraro, and F. Porcelli, Phys. Lett. A 132, 267 (1988).
[19] F. Zonca, L. Chen, Physics of Plasmas 21, 072120 (2014)

[20] F. Zonca, L. Chen, Physics of Plasmas 21, 072121 (2014)
[21] X. Garbet, PhD thesis, Annex A, 1988
[22] A.N. Kaufman, Phys. FLuids, 15, 1063 (1972)
[23] H.E. Mynick and J.A. Krommes, Phys. Rev. Lett. 43, 1506 (1979)
[24] A.J.Brizard, T.S.Hahm, Reviews of modern physics, 79, 2007
[25] J. Graves, Plasma Phys. Control. Fusion 55 (2013) 074009
[26] H. Lütjens, A. Bondeson, O. Sauter, Computer Physics Communications 97 (1996) 219-260
[27] H. Lütjens, J-F. Luciani, JCP, (2010), 229, 8130-8143
[28] B. Davies, Journal of Computational Physics 66, 3649 (1986)
[29] F. Porcelli, R. Stankiewicz, H. L. Berk, Y. Z. Zhang, Phys. FLuid B 4 (10), 1992